

N O T I C E

THIS DOCUMENT HAS BEEN REPRODUCED FROM
MICROFICHE. ALTHOUGH IT IS RECOGNIZED THAT
CERTAIN PORTIONS ARE ILLEGIBLE, IT IS BEING RELEASED
IN THE INTEREST OF MAKING AVAILABLE AS MUCH
INFORMATION AS POSSIBLE

University of Missouri-Rolla

Rolla, Missouri 65401

(NASA-CR-162897) TRANSPORT PROPERTIES IN
THE ATMOSPHERE OF JUPITER Semiannual
Progress Report, Jul. - Dec. 1979 (Missouri
Univ. -Rolla.) 35 p HC A03/MF A01 CSCL 03B

N80-21234

Unclas

G3/91 46742

TRANSPORT PROPERTIES IN THE ATMOSPHERE OF JUPITER

Semi-Annual Progress Report

July-December, 1979

NASA Research Grant NSG 1369

Louis Biolsi, Jr.
Chemistry Department



The work accomplished during this reporting period falls into the following categories; (1) testing of the computer program used to obtain transport properties for the Hulburt-Hirschfelder potential, (2) calculation of transport properties for the C-C interaction, (3) rough estimates for transport properties for the important ablation species, and (4) estimates of transport properties for some of the species associated with photochemical smog. The results are discussed in sections I through IV below.

I. TEST OF THE HULBURT-HIRSCHFELDER POTENTIAL

It was previously reported¹ that a computer program has been written to calculate transport collision integrals for the Hulburt-Hirschfelder (H-H) potential.^{2,3} This potential is probably the most accurate general purpose potential for representing atom-atom interactions. It consistently gives as good or better agreement with the "experimental" Rydberg-Klein-Rees (RKR) potential energy curve^{1,4} as any other general purpose potential.^{5,6,7} The H-H potential also has the ability to reproduce the local maximum in the potential energy curve often found for atom-atom interactions.^{8,9,10,11}

The comparison of H-H and RKR potential energy curves provides one test of the H-H potential. A further test of this potential is provided by using it to calculate bulk data such as transport properties and virial coefficients and comparing these results with the experimental results. It was previously reported¹² that viscosity coefficients had been calculated for argon using the H-H potential. These calculations have been extended and the diffusion and thermal conductivity coefficients of argon have also been calculated. A modified version of the O'Hara-Smith program¹³ was used for these calculations. The results of these calculations are shown in Figures 1, 2 and 3.

In addition, second virial coefficients have been calculated for argon using the H-H potential. A modified version of a previous program^{14,15} was used for these calculations. The results are shown in Figure 4.

The excellent agreement between the calculated and experimental results for the transport properties over a wide temperature range reinforces the conclusion drawn from direct comparisons of the H-H and RKR potential energy curves; i.e. the H-H potential appears to be an excellent model potential for atom-atom interactions. It is important to emphasize that this agreement has been obtained in spite of the fact that the H-H potential contains no adjustable parameters. All constants in the potential are determined from the measured spectroscopic constants which are known for the ground $1\Sigma_g^+$ state of Ar_2 ^{16,17}. Thus there are no "fudge factors" in the H-H potential which can be used to adjust the fit of the calculated to the experimental results.

Figures 1-3 indicate that the differences between the calculated and experimental transport properties tend to be largest at low temperatures. This effect is most pronounced for the viscosity. The effect is probably best explained by examining the H-H potential in more detail. The constants in the H-H potential were obtained by using the Dunham method^{2,18,19} which is based on the use of a polynomial expansion that does not converge⁶ at large values of r . Thus one would expect that, in general, the H-H potential will not give a highly accurate representation of the long range part (tail) of the potential. At low temperatures, the contribution of the tail of the potential to the transport properties is greater than at higher temperatures, especially for the viscosity.^{20,21,22} Thus the greater differences between calculated and experimental results at low temperatures are expected. Since the long range forces between neutral, nonpolar species are dispersion forces,^{20,21} which are quantum mechanical in origin, this is a quantum mechanical effect.

The percentage deviation for the second virial coefficient is much larger than for the transport properties over a very wide temperature range. This

was also a result of the calculations of Hanley and Klein.²³ The reason for this can be seen by comparing the H-H potential energy curve with the RKR curve¹⁷ for Argon. To do this, define

$$V^*(\text{H-H}) = \frac{V_{\text{HH}}(r)}{91.6 \text{ cm}^{-1}}, \quad V^*(\text{RKR}) = \frac{V_{\text{RKR}}(r)}{99.55 \text{ cm}^{-1}}$$

The ratio $V^*(\text{H-H})/V^*(\text{RKR})$ is given in Table 1. The agreement is quite good near r_e where both the H-H and RKR results should be most accurate.

At small values of r , the H-H results are larger; i.e. the repulsive potential wall is steeper for the H-H potential. Since the RKR results at small values of r were obtained by constraining the results obtained from the data to fit a Morse curve¹⁷, it is difficult to ascertain a priori if the H-H or RKR results are more reliable in this region. However, at moderate temperatures, the transport properties of the inert gases are almost completely determined by the repulsive wall of the potential while second virial coefficients depend also on the outer part of the potential.²² This is a consequence of the fact that "close" collisions are necessary for the transfer of energy and/or momentum associated with the transport properties while long range "soft" van der Waals type interactions are more important for the virial coefficients. The good fit of the calculated to the experimental transport properties over a wide range of temperature indicates that the repulsive wall is reasonably accurately determined for the H-H potential. This is to be expected since the good spectroscopic fit near r_e should help to constrain the H-H curve so that accurate results are obtained for the nearby repulsive wall.

Table 1 shows that, at large values of r , the H-H results are again higher than the RKR results; i.e. the RKR potential is longer range. Since Colbourn and Douglas¹⁷ obtained the long range RKR results by a careful comparison with

second virial coefficient data, the RKR results are almost certainly more accurate in this region. This helps explain the relatively poor results obtained for the second virial coefficient using the H-H potential; i.e. the good spectroscopic fit at r_e is not able to constrain the H-H curve at large distances well enough to assure that virial coefficients will be accurately predicted.

The large low temperature deviations of the virial coefficient are probably due to quantum mechanical effects since it is known that quantum mechanical effects are much larger for virial coefficients than for transport properties.²² However, this is not likely to be due almost solely to dispersion forces, as for transport properties, since, for the rare gases, there is no temperature range over which the second virial coefficient is determined solely by the tail of the potential.²³

In summary, the H-H potential appears to accurately represent the "true" atom-atom potential over a wide enough range of interatomic separations so that the transport properties can be accurately estimated over a wide temperature range without the need to empirically adjust any of the experimentally determined spectroscopic constants used in the potential. The second virial coefficient can probably only be accurately predicted at high temperatures where it is relatively insensitive to the tail of the potential. It should be emphasized that the great utility of the H-H potential lies in its ability to estimate bulk properties for systems involving atom-atom interactions for which these properties are difficult or impossible to measure. The JANAF Thermochemical Tables²⁴ and the compilation of Huber and Herzberg²⁵ provide the required spectroscopic constants for many atom-atom interactions.

II. TRANSPORT PROPERTIES FOR THE C-C INTERACTION

The recalculation of the C-C transport properties, using the H-H potential for the bound states of C_2 , has been discussed in previous reports.^{1,12} In addition, two states ignored in the original calculations²⁶ were included in the calculation by using the perfect pairing method.^{1,5,21,27} These calculations have now been completed. Results for the diffusion collision integral, $\sigma_{\Omega}^{2,0}(1,1)^*$, and the viscosity collision integral, $\sigma_{\Omega}^{2,0}(2,2)^*$, are shown in Table 2.

A comparison of the results in Table 2 with the previous results for the collision integrals²⁶ shows that the differences are quite substantial (in some cases the collision integrals differ by more than 50%). There are three reasons for these differences;

1. use of the H-H potential, rather than the Morse potential, to represent the states with a potential minimum,
2. inclusion of collision integrals for the $3\chi_{u2}^+$ and $5\chi_{g2}^+$ states which were ignored in the previous calculation,²⁶ and
3. optimization of the collision integrals for the repulsive states by using the method of Hirschfelder and Eliason²⁸ to determine which range of interatomic separations makes most of the contribution to the transport collision integrals for a given temperature range.

This optimization technique requires some explanation. For a given temperature, it is observed that most of the contribution to the transport collision integrals comes from a region of the intermolecular potential representing a narrow range of interatomic separations.²⁸ In the limiting case of a rigid sphere potential, all of the contribution to the collision integrals comes from a single interatomic separation; i.e. the rigid sphere diameter, σ_{rs} . Based on the observation mentioned above and the fact that a rigid sphere model gives a good first approximation to the transport collision integrals for

atom-atom interactions (and for most other interactions as well), Hirschfelder and Eliason²⁸ proposed calculating an equivalent rigid sphere diameter, σ_{ers} , using the collision integrals, $\sigma_{BB}^{2\Omega}(a,b)^*$, determined for some assumed interaction potential which gives the best fit to available experimental and/or theoretical information. The equivalent rigid sphere diameter is calculated from²⁸

$$\sigma_{ers}^2(T) = \sigma_{BB}^{2\Omega}(a,b)^*(T) \quad (1)$$

For the repulsive states of C_2 , the $\sigma_{BB}^{2\Omega}(a,b)^*$ were determined for the exponential repulsive potential²⁹, using the potential parameters determined by making a best fit of this potential to the theoretical calculations of Fougere and Nesbet¹¹ and to the results of the perfect pairing calculations.¹

According to Hirschfelder and Eliason,²⁸ the region of the potential in the vicinity of $\sigma_{ers}(T)$, as determined from equation (1), should be the region of the potential that makes most of the contribution to the transport collision integrals. Thus σ_{ers} was calculated at 1000°K and 25,000°K, using equation (1) and the viscosity collision integral, $\sigma_{BB}^{2\Omega}(2,2)^*$ (since thermal conductivity is the transport property of greatest interest), to find the range of σ_{ers} as a function of temperature. Then the exponential repulsive potential was reoptimized so that the best fit to the theoretical results was obtained over the range of σ_{ers} as determined from equation (1). Then a new set of collision integrals was determined for the reoptimized parameters. Then a new range of σ_{ers} was determined, using equation (1), etc. This iteration procedure was repeated until there was no change in the σ_{ers} . The last iteration was assumed to be the best fit of the exponential repulsive potential to the theoretical results and the transport collision integrals were calculated²⁹ using the parameters obtained for the last iteration.

Some of the difference between the results for the transport collision integrals in Table 2 and the previous results²⁶ is due to the optimization of the curve fit of the empirical to the calculated repulsive potential over the temperature range of interest, as discussed above, and some of the difference is due to the inclusion of two states that were previously ignored. However, most of the difference is due to the use of the H-H potential, rather than the Morse potential, to represent the potential energy curves with an attractive minimum. Since the H-H potential usually gives better agreement with the RKR results than does the Morse potential, these results for the transport collision integrals are considerably more reliable than the results reported previously.²⁶

One interesting result of the C_2 study is the possibility that, in some cases, the H-H potential may be more accurate than the RKR potential. In general, the H-H results give better agreement with the RKR results than do the Morse results. This is illustrated in Table 3 for the $^3\Pi_u$ state. However, the agreement is reversed for the $^1\Pi_g$ state at large separations, as shown in Table 3. The RKR and Morse results predict that this state does not have a local maximum (hump) while the H-H results predict a hump. The theoretical calculations of Fougere and Nesbet¹¹ also predict that this state has a hump. The best available evidence indicates^{11,30} that the $^1\Pi_g$ state should have a hump in order to avoid crossing another $^1\Pi_g$ potential energy curve. Thus it appears that, for the $^1\Pi_g$ state of C_2 , the H-H results are more reliable than the RKR results at large separations. This is not surprising since, as discussed previously, errors are introduced into the RKR results at large separations. Nevertheless, this result is satisfying and provides additional evidence of the reliability of the H-H potential.

III. TRANSPORT PROPERTIES USING "UNIVERSAL" COLLISION INTEGRALS

The composition at the surface of a probe upon entry into the Jovian atmosphere is given³¹ in Table 4. The "atmosphere" represented by the species listed in Table 4 is entirely due to the presence of ablative species. Note that the mole fraction of these species is unity to four significant figures; i.e. these species account for essentially the entire atmosphere at the surface of the entry probe.

At the request of Dr. J. N. Moss, an estimate was made of the transport collision integrals for the species listed in Table 4. While the procedure used is relatively crude, the estimates should be more reliable than those based on the method proposed by Esch, et al.,³² the only previous attempt of which the author is aware to calculate the transport properties of ablation products using the kinetic theory of gases.

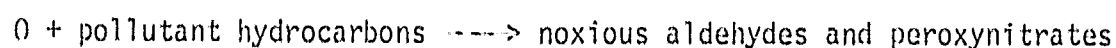
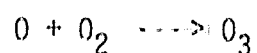
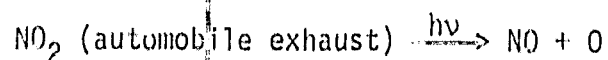
The "universal" set of collision integrals obtained by Boushehri, et al.²² have been used to estimate the transport collision integrals for the species listed in Table 4. The primary justification for the assumption that these collision integrals can be applied to a wide variety of interactions is the observation²² that the transport properties of the rare gases are relatively insensitive to the details of the interaction potential; i.e. the repulsive wall of the potential (which tends to vary little from interaction to interaction) makes the primary contribution to the transport collision integrals. This set of collision integrals has been applied to a variety of atom-molecule and molecule-molecule interactions^{22,33,34,35,36,37} with good results. However, one cannot be certain that these collision integrals are applicable to any given interaction and workers in the field with whom the author has communicated are skeptical about the general applicability of this method. Nevertheless, this is probably the best method available for estimating transport collision

integrals in the absence of detailed information about interaction potentials. Also, at the high temperatures attained during Jovian entry, the repulsive part of the potential should make the primary contribution to the transport properties, increasing the reliability of the universal collision integrals.²²

In order to use these collision integrals, estimates of σ , the effective rigid sphere diameter, and r , the depth of the potential well, are needed. The estimates of these parameters obtained by Esch, et al.³² were used in the calculations. These are given in Table 5. The resulting diffusion collision integrals are given in Table 6 and the viscosity collision integrals are given in Table 7.

IV. TRANSPORT PROPERTIES ASSOCIATED WITH PHOTOCHEMICAL SMOG

The basic chemical equations associated with the production of photochemical smog from automobile emissions are³⁸



Transport properties have been estimated for the species given in the first two chemical reactions listed above. The two body interactions involving these species are listed in the first column of Table 3.

A variety of techniques were used to estimate the interaction potentials and transport properties for these interactions. The empirical interaction potentials used are the exponential repulsive (ER) potential; i.e.

$$V(r) = A e^{-Dr} \quad (2)$$

the exponential-six (ES) potential; i.e.

$$V(r) = \frac{1}{(1-6/4)} \left[\frac{6}{r_0} e^{-\alpha(1-r/r_0)} - \left(\frac{r_0}{r}\right)^6 \right] \quad (3)$$

and the inverse power attractive (IA) potential; i.e.

$$V(r) = -\frac{B}{r^S} \quad (4)$$

For a number of the interactions listed in Table 8, the peripheral force method⁴⁰ was used to obtain atom-molecule and molecule-molecule interactions from atom-atom interactions. The basic atom-atom interactions used are

$$V(r) = -\frac{124.5}{r^{7.83}} \text{ (ev)} \quad (5)$$

for the O-O interaction between two ground state ($^3\Sigma_g^-$) atoms³⁹,

$$V(r) = -\frac{98.09}{r^{6.38}} \text{ (ev)} \quad (6)$$

for the N-N interaction between two ground state ($^1\Sigma_g^+$) atoms³⁹, and

$$V(r) = -\frac{105.9}{r^{7.00}} \text{ (ev)} \quad (7)$$

for the N-O interaction for NO in its lowest state ($^2\Pi$).³⁹ These potentials were used to obtain orientation averaged atom-molecule and molecule-molecule potentials according to the peripheral force method.^{1,12,40} The interactions for which the peripheral force method has been used are listed in the second column of Table 8 with the label PF. These orientation averaged potentials were then best fit with the IA potential. The best fit parameters are shown in the third column of Table 8.

The peripheral force method does not work well for some of the interactions. This has been discussed previously.^{41,42} For these interactions, the "universal"

collision integrals recommended by Boushehri, et al.²² have been used to calculate the transport properties. The use of this technique is denoted in the second column of Table 8 by the label B. The required values of σ and ϵ were obtained from tabulations for the Lennard-Jones (6,12) potential or σ was estimated from bond lengths using a "rigid sphere model" and ϵ was estimated from polarizabilities.²⁰

The O-O transport collision integrals were extrapolated to lower temperatures from the tables provided by Yun and Mason³⁹ and the potentials suggested by Yun and Mason³⁹ were used for the O-O₂ and O₂-O₂ interactions. The parameters obtained for the various interaction potentials are shown in the third column of Table 8.

The calculation of the transport properties has been discussed previously.^{20,43} Some sample results are shown in Tables 9 and 10. These results are not intended to be definitive since improvements in several of the assumed potentials are possible. However these results do suggest that some of the techniques being used to calculate the effects of ablation products on the transport properties are also useful for other practical calculations.

ORIGINAL PAGE IS
OF POOR QUALITY

References

1. L. Biolsi, NASA Semi-annual report, Dec., 1978.
2. H. M. Hulburt and J. O. Hirschfelder, J. Chem. Phys. 9, 61 (1941).
3. H. M. Hulburt and J. O. Hirschfelder, J. Chem. Phys. 35, 1901 (1961).
4. J. T. Vanderslice, E. A. Mason, and W. G. Maisch, J. Mol. Spec. 3, 17 (1959).
5. J. T. Vanderslice, E. A. Mason, and W. G. Maisch, J. Chem. Phys. 32, 515 (1960).
6. D. Steele, E. R. Lippincott, and J. T. Vanderslice, Rev. Mod. Phys. 34, 239 (1962).
7. G. C. Lie and I. Clementi, J. Chem. Phys. 60, 1283 (1974).
8. R. S. Mullikan, J. Phys. Chem. 41, 5 (1937).
9. G. Herzberg, "Molecular Spectra and Molecular Structure, Vol. 1. Spectra of Diatomic Molecules", Van Nostrand, Princeton, 1950.
10. J. C. Browne and F. A. Matsen in "Advances in Chemical Physics - Vol. XXIII", I. Prigogine and S. A. Rice (eds.), Interscience, New York, 1973.
11. P. F. Fougere and R. K. Nesbet, J. Chem. Phys. 44, 285 (1966).
12. L. Biolsi, NASA, Semi-annual report, June, 1979.
13. H. O'Hara and F. J. Smith, Comput. Phys. Commun. 2, 47 (1971).
14. J. F. Ely and H.J.M. Hanley, Mol. Phys. 30, 565 (1975).
15. P. M. Holland, J. F. Ely, and H.J.M. Hanley, J. Res. Nat. Bur. Stand. 82, 123 (1977).
16. Y. Tanaka and K. Yoshino, J. Chem. Phys. 53, 2012 (1970).
17. E. A. Colbourn and A. E. Douglas, J. Chem. Phys. 65, 1741 (1976).
18. J. L. Dunham, Phys. Rev. 41, 713, 721 (1932).
19. A. S. Coolidge, H. M. James, and E. L. Vernon, Phys. Rev. 54, 726 (1938).
20. J. O. Hirschfelder, C. F. Curtiss, and R. B. Bird, "Molecular Theory of Gases and Liquids", Wiley, New York, 1954.
21. E. A. Mason and L. Monchick in "Advances in Chemical Physics. Vol. 12, Intermolecular Forces", J. O. Hirschfelder (ed.), Interscience, New York, 1967.

22. A. Poushehri, L. A. Viehland, and E. A. Mason, *Physica* 91A, 424 (1978).
23. H.J.M. Hanley and M. Klein, *J. Phys. Chem.* 76, 1743 (1972).
24. D. R. Stull and H. Prophet (eds.), "JANAF Thermochemical Tables", NSRDS-NBS 37, 1971.
25. K. P. Huber and G. Herzberg, "Molecular Spectra and Molecular Structure, Vol. IV, Constants of Diatomic Molecules", Van Nostrand, New York, 1979.
26. L. Biolsi, *J. Geophys. Res.* 83, 2476 (1978).
27. J. T. Vanderslice, E. A. Mason, and E. R. Lippincott, *J. Chem. Phys.* 30, 129 (1959).
28. J. O. Hirschfelder and M. Eliason, *N.Y. Acad. Sci. Monogr.* 67, 451 (1967).
29. L. Monchick, *Phys. Fluids* 2, 695 (1959).
30. E. A. Ballik and D. A. Ramsey, *Astrophys. J.* 137, 84 (1963).
31. J. N. Moss, private communication.
32. D. D. Esch, A. Sirinpong, and R. W. Pike, CR-111989, NASA, 1970.
33. J. Kestin, S. T. Ro, and W. A. Wakeham, *J. Chem. Phys.* 56, 4119 (1972).
34. J. Kestin, H. E. Khalifa, S. T. Ro, and W. A. Wakeham, *Physica* 08A, 242 (1977).
35. J. M. Hellemans, J. Kestin, and S. T. Ro, *J. Chem. Phys.* 57, 4038 (1972).
36. J. M. Hellemans, J. Kestin, and S. T. Ro, *Physica* 65, 362 (1973).
37. J. M. Hellemans, J. Kestin, and S. T. Ro, *Physica* 65, 376 (1973).
38. A. W. Adamson, "A Textbook of Physical Chemistry", Academic Press, New York, 1973.
39. K. S. Yun and E. A. Mason, *Phys. Fluids* 5, 380 (1962).
40. I. Amdur, E. A. Mason, and J. E. Jordan, *J. Chem. Phys.* 27, 527 (1957).
41. I. Amdur, W. A. Peters, J. E. Jordan, and E. A. Mason, *J. Chem. Phys.* 64, 1538 (1976).
42. C.R.A. Catlow, A. H. Harker, and M. R. Hayns, *J. Chem. Soc. (Far. Trans. II)* 71, 275 (1975).
43. L. Biolsi, *J. Geophys. Res.* 83, 1125 (1978).
44. G. C. Maitland and E. B. Smith, *J. Chem. Eng. Data* 17, 150 (1972).

45. W. G. Kammluik and E. H. Carman, Proc. Phys. Soc. (London) B65, 701 (1952).
46. H. Ziebland and J.T.A. Burton, Brit. J. Appl. Phys. 9, 52 (1958).
47. K. L. Schaeffer and F. W. Reiter, Naturwiss. 43, 296 (1956); Z. Electrochem. 61, 230 (1957).
48. A. Michels, J. V. Sengers, and L.J.M. Van de Klundert, Physica 29, 149 (1963).
49. E. B. Winn, Phys. Rev. 80, 1024 (1950).
50. F. Hutchinson, J. Chem. Phys. 17, 1081 (1949).
51. H. F. Vugts, A.J.H. Boerboom, and J. Los, Physica 44, 219 (1969).
52. M. De Paz, B. Turi, and M. L. Klein, Physica 36, 127 (1957).
53. J.M.H. Levelt Sengers, M. Klein, and J. S. Gallagher in "American Institute of Physics Handbook", 3rd ed., D. E. Gray (ed.), McGraw-Hill, New York, 1972.

Table 1

Ratio of the Reduced H-H Potential to the Reduced RKR Potential for Ar₂

$r(\text{\AA})$	$V^*(\text{H-H})/V^*(\text{RKR})$	$r(\text{\AA})$	$V^*(\text{H-H})/V^*(\text{RKR})$
3.300	1.278	4.350	0.952
3.350	5.526	4.400	0.942
3.400	0.815	4.450	0.933
3.450	0.916	4.500	0.923
3.500	0.961	4.600	0.901
3.550	0.981	4.700	0.879
3.600	0.989	4.800	0.860
3.650	0.994	4.900	0.829
3.700	0.998	5.000	0.795
3.750	1.000	5.100	0.762
3.800	1.000	5.200	0.738
3.850	0.999	5.300	0.709
3.900	0.997	5.400	0.673
3.950	0.995	5.600	0.601
4.000	0.993	5.800	0.534
4.050	0.991	6.100	0.437
4.100	0.987	6.400	0.351
4.150	0.982	6.700	0.279
4.200	0.976	7.100	0.198
4.250	0.969	7.500	0.142
4.300	0.961		

The RKR results are from Colbourn and Douglas.¹⁷

Table 2

Transport Collision Integrals for the C-C Interaction

$T \times 10^{-3} (^{\circ}\text{K})$	$\Omega_{\Omega}^{2,2}(1,1)^*$	$\Omega_{\Omega}^{2,2}(2,2)^*$
1	7.0296	8.2429
2	5.9531	6.9545
3	5.4100	6.2927
4	5.0414	5.8495
5	4.7117	5.5228
6	4.6049	5.2607
7	4.4820	5.0516
8	4.2092	4.8695
9	4.0649	4.7120
10	3.9327	4.5690
11	3.8171	4.4429
12	3.7099	4.3291
13	3.6091	4.2205
14	3.5144	4.1188
15	3.4238	4.0220
16	3.3362	3.9315
17	3.2552	3.8453
18	3.1795	3.7630
19	3.1074	3.6873
20	3.0401	3.6124
21	2.9754	3.5418
22	2.9136	3.4719
23	2.8547	3.4061
24	2.7990	3.3414
25	2.7455	3.2818

The collision integrals are in \AA^2

Table 3

RKR, H-H, and Morse Potential (MP) Energy Results
for the ${}^3\Pi_u$ and ${}^1\Pi_g$ States of C_2

$r(\text{\AA})$	$V(\text{RKR})$	$V(\text{HH})$	$V(\text{MP})$	$r(\text{\AA})$	$V(\text{RKR})$	$V(\text{HH})$	$V(\text{MP})$
1.098	2.15	2.17	2.27	1.103	1.20	1.38	1.48
1.105	1.98	1.99	2.09	1.111	1.08	1.19	1.28
1.113	1.80	1.81	1.89	1.120	0.922	1.00	1.09
1.121	1.62	1.64	1.71	1.132	0.740	0.790	0.856
1.131	1.44	1.44	1.50	1.148	0.541	0.564	0.605
1.141	1.26	1.25	1.31	1.169	0.330	0.341	0.358
1.152	1.08	1.07	1.12	1.202	0.112	0.119	0.119
1.164	0.886	0.891	0.929	1.313	0.112	0.109	0.090
1.179	0.695	0.696	0.724	1.365	0.330	0.344	0.267
1.197	0.500	0.500	0.519	1.405	0.541	0.575	0.429
1.221	0.302	0.297	0.308	1.444	0.740	0.815	0.593
1.257	0.101	0.100	0.103	1.488	0.922	1.08	0.775
1.374	0.101	0.101	0.102	1.545	1.08	1.40	0.994
1.425	0.302	0.303	0.305	1.621	1.20	1.73	1.25
1.463	0.500	0.501	0.502				
1.495	0.695	0.691	0.690				
1.525	0.886	0.884	0.880				
1.553	1.08	1.07	1.06				
1.580	1.26	1.26	1.25				
1.605	1.44	1.44	1.42				
1.630	1.62	1.61	1.59				
1.655	1.80	1.79	1.76				
1.679	1.98	1.96	1.93				
1.702	2.15	2.13	2.08				

Potential energy is in electron volts. The RKR results are from Read and Vanderslice.

Table 4
Mole Fractions of the Gaseous Species at the Surface of a Probe During
Jovian Entry for Stagnation-Point Peak Heating

Species	Mole Fraction
C_3	0.303
H	0.149
C_4H	0.138
C_2H	0.115
CO	0.108
C_3H	0.099
C_2	0.028
C	0.026
H_2	0.024
C_2H_2	0.010
Total	1.000

Table 5

The Parameters ϵ/k and σ to be Used With the Set of Universal Collision Integrals

<u>Species</u>	<u>ϵ/k ($^{\circ}\text{K}$)</u>	<u>σ (\AA)</u>
C_3	128.0	4.450
C_4H	504.0	5.210
C_2H	205.0	3.880
C_3H	356.0	4.600
C_2H_2	231.8	4.033

The parameters are from Esch, et al.³²

Table 6

The Diffusion Collision Integrals, $\sigma_{\Omega}^2(1,1)^*$, for the C_3-C_3 , C_4H-C_4H ,
 C_2H-C_2H , C_3H-C_3H , and $C_2H_2-C_2H_2$ Interactions

$T \times 10^{-3}$ (°K)	$\sigma_{\Omega}^2(1,1)^*$ in Å ²				
	C_3	C_4H	C_2H	C_3H	C_2H_2
1	15.30	29.71	12.78	20.67	14.20
2	13.46	24.15	11.16	17.45	12.33
3	12.49	22.11	10.36	16.12	11.45
4	11.82	20.90	9.83	15.28	10.86
5	11.32	20.05	9.42	14.67	10.42
6	10.91	19.40	9.10	14.19	10.07
7	10.58	18.86	8.83	13.79	9.77
8	10.29	18.40	8.60	13.45	9.52
9	10.05	18.01	8.41	13.15	9.31
10	9.83	17.66	8.23	12.89	9.11
11	9.63	17.35	8.07	12.66	8.94
12	9.45	17.07	7.93	12.45	8.78

Table 7

The Viscosity Collision Integral, $\sigma_{\omega}^{2,2}(2,2)^*$, for the C_3-C_3 , C_4H-C_4H ,
 C_2H-C_2H , C_3H-C_3H , and $C_2H_2-C_2H_2$ Interactions

$T \times 10^{-3}$ ($^{\circ}K$)	$\sigma_{\omega}^{2,2}(2,2)^*$ in \AA^2				
	C_3	C_4H	C_2H	C_3H	C_2H_2
1	17.09	32.12	14.13	22.58	15.66
2	15.50	26.59	12.54	19.35	13.82
3	14.31	24.56	11.76	18.04	12.95
4	13.02	23.37	11.22	17.23	12.37
5	13.09	22.55	10.81	16.63	11.92
6	12.65	21.91	10.47	16.15	11.56
7	12.29	21.37	10.19	15.75	11.25
8	11.97	20.92	9.95	15.40	10.99
9	11.70	20.52	9.74	15.10	10.76
10	11.45	20.17	9.55	14.83	10.55
11	11.23	19.85	9.38	14.58	10.37
12	11.02	19.56	9.22	14.36	10.20

Table 8

Interaction Potentials for the Species Associated with Photochemical Smog

Interaction	Potential	Parameters*
O-O	Many ³⁹	
O-O ₂	E.R. ³⁹	A=2162, $\rho=3.479$
O ₂ -O ₂	E.S. ³⁹	$\alpha=17$, $\epsilon=0.0114$, $r_e=3.726$
O-O ₃	I.A. (P.F.)	$B=7.260 \times 10^5$, $s=13.49$
O-NO	I.A. (P.F.)	$B=1347$, $s=8.67$
O-NO ₂	I.A. (P.F.)	$B=4.956 \times 10^5$, $s=13.67$
NO-NO	I.A. (P.F.)	$B=3.871 \times 10^4$, $s=11.08$
NO-NO ₂	B	
NO ₂ -NO ₂	B	
O ₂ -NO	B	
O ₂ -NO ₂	B	
O ₃ -NO	B	
O ₃ -NO ₂	B	
O ₂ -O ₃	B	
O ₃ -O ₃	B	

*The parameters are chosen so that potential energy is in electron volts.

Table 9

Transport Properties of the Pure Species Associated with Photochemical Smog
and the Binary Diffusion Coefficient

Interaction	D_{ij} (cm ² /sec)	η (μ P)	λ_{tr} (W/m/ $^{\circ}$ K)	λ_{int} (W/m/ $^{\circ}$ K)
O-O	0.305	0.17	0.034	0
O ₂ -O ₂	0.148	0.18	0.017	0.006
O ₃ -O ₃	0.428	0.74	0.048	0.018
NO-NO	0.145	0.16	0.016	0
NO ₂ -NO ₂	0.392	0.66	0.045	0.016
O-O ₂	0.229			
O-O ₃	0.170			
O ₂ -O ₃	0.243			
O-NO	0.174			
O-NO ₂	0.188			
O ₂ -NO	0.143			
O ₂ -NO ₂	0.238			
O ₃ -NO	0.246			
O ₃ -NO ₂	0.421			
NO-NO ₂	0.231			

These results are for a temperature of 250⁰K.

Table 10
 Thermal Conductivity, λ (W/m⁰K), of the Mixture of Species Associated with
 Photochemical Smog

T (°K)	λ_{tr}^{mix}	λ_{int}^{mix}	λ_{tr+int}^{mix}	$\lambda_{reactive}$
200	0.018	0.010	0.028	0.468
250	0.021	0.006	0.027	0.135
300	0.024	0.012	0.036	0.202

These results were calculated by assuming that the mole fractions of all species were the same.

Figure 1

Percentage deviation plot of the experimental viscosity of argon compared to the viscosity calculated from the H-H potential. Data from: \diamond (33); \circ (44).

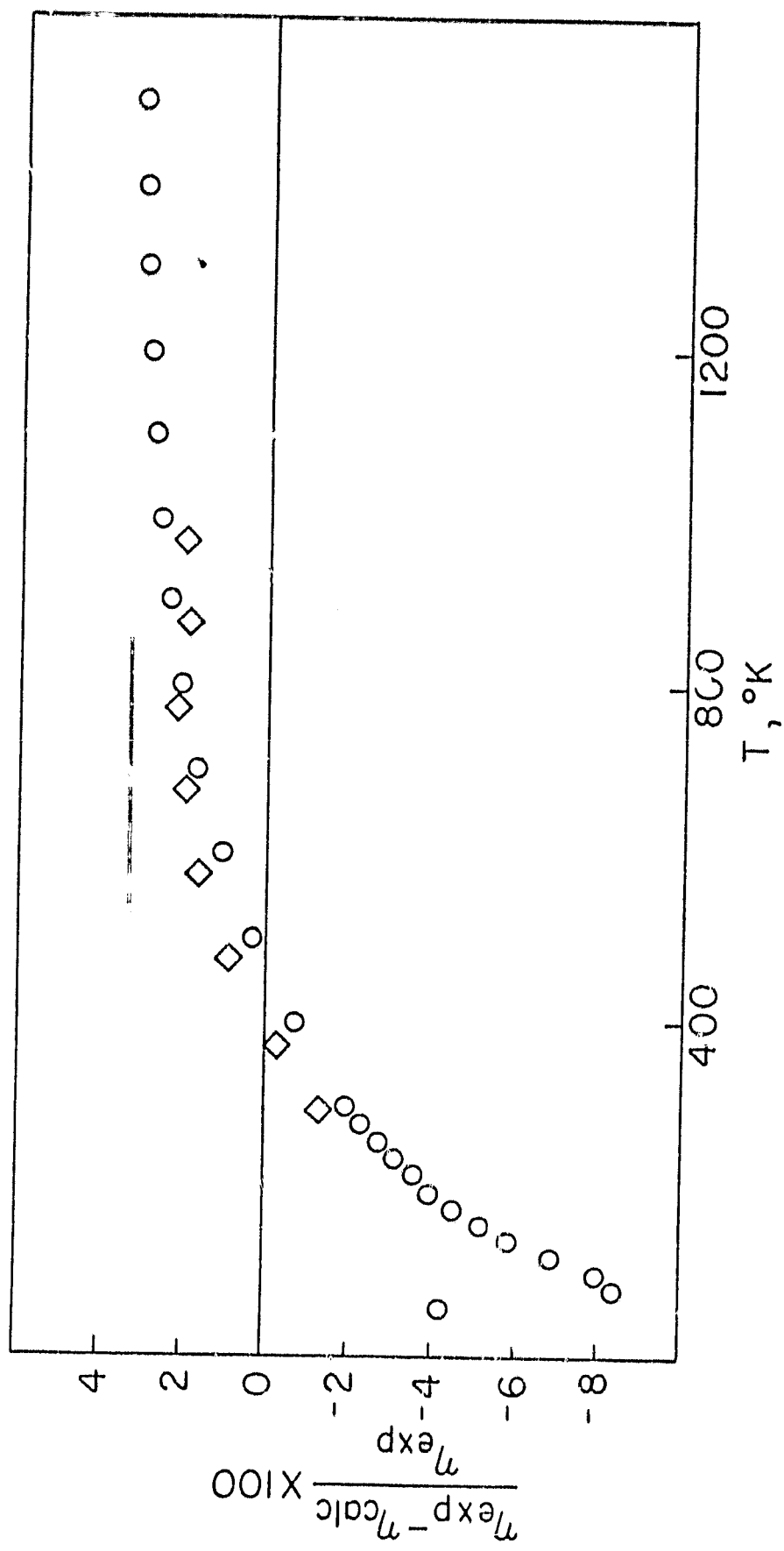


Figure 2

Percentage deviation plot of the experimental thermal conductivity of argon compared to the thermal conductivity calculated from the H-H potential. Data from: \diamond (45); \cdot (46); Δ (47); \circ (48).



Figure 3

Percentage deviation plot of the experimental diffusion coefficient of argon compared to the diffusion coefficient calculated from the II-II potential. Data from: \diamond (49); \cdot (50); Δ (51); \circ (52). The data in reference 31 are relative to the diffusion coefficient at 298.15°K. This value, 0.182 cm²/sec, was calculated using the exponential-six potential (see reference 31).

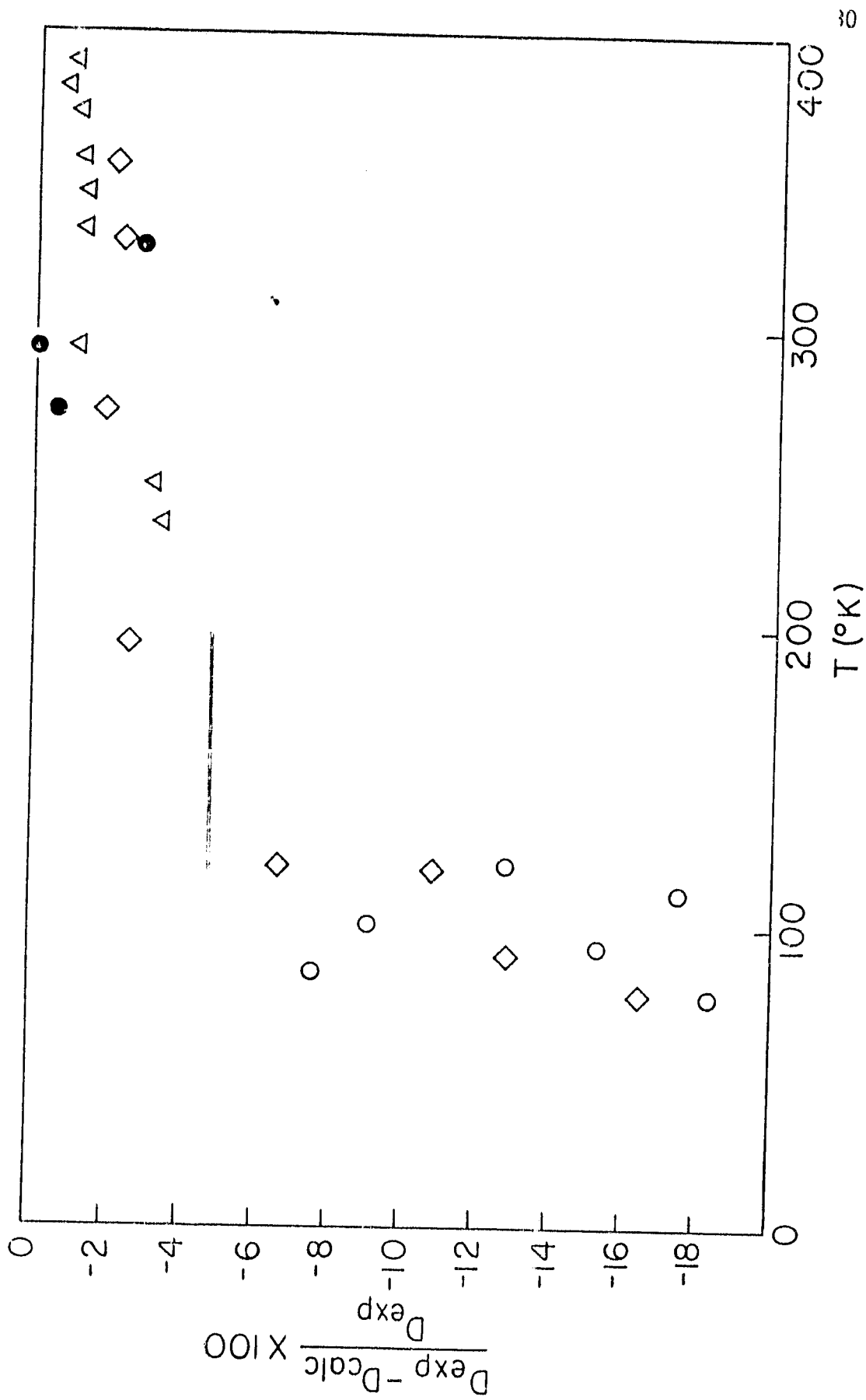
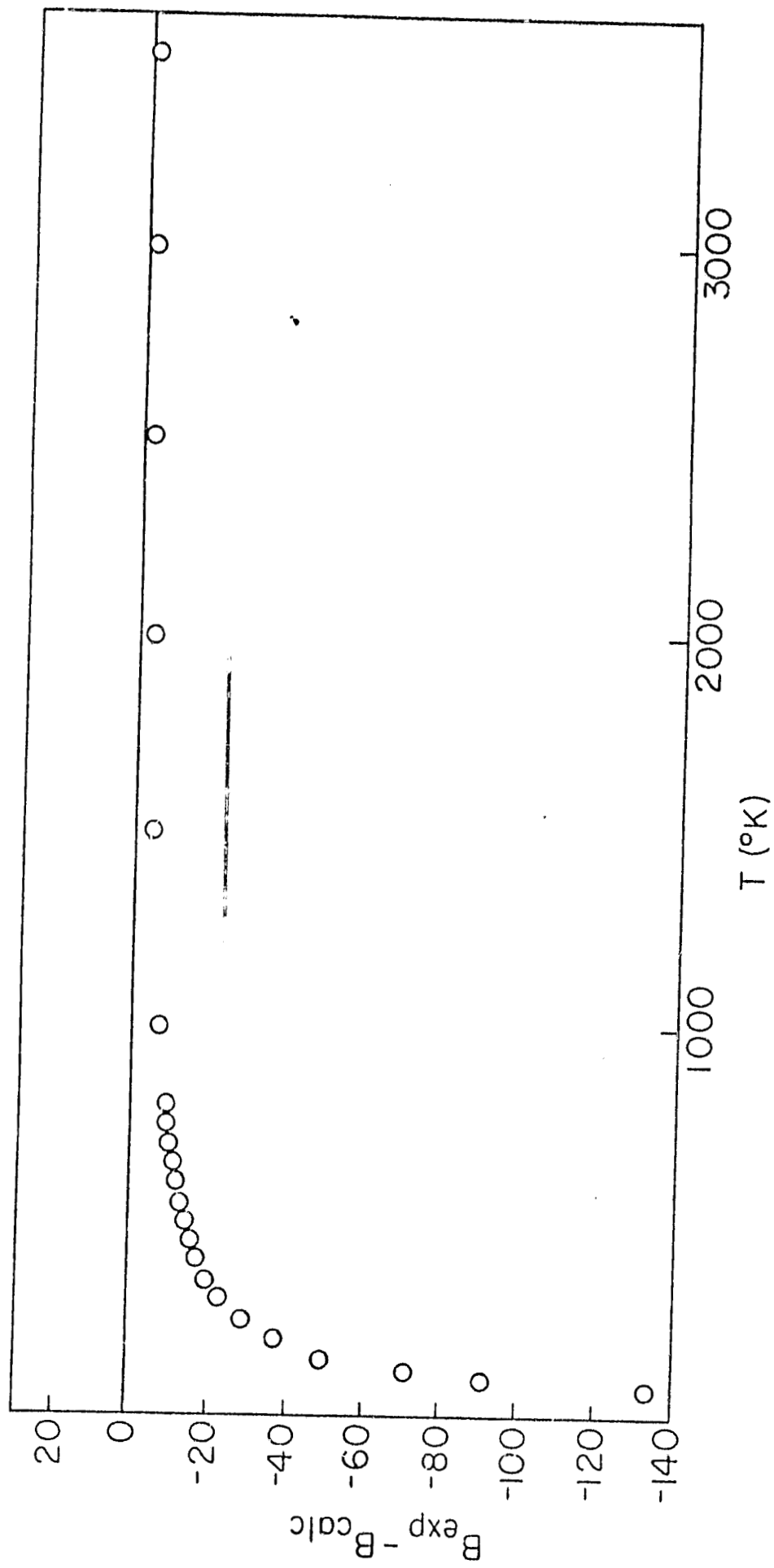


Figure 4

Deviation plot of the experimental second virial coefficient of argon compared to the second virial coefficient calculated from the H-II potential. Data from: o (53).



Publications

- L. Biolsi
"Transport Properties in the Jovian Atmosphere"
Journal of Geophysical Research, 83, 1125 (1978).
- L. Biolsi
"Transport Properties of Monatomic Carbon"
Journal of Geophysical Research, 83, 2476 (1978).
- L. Biolsi and L. R. Wallace
"Some Effects of Ablation on Transport Properties in the Jovian Atmosphere"
Progress in Astronautics and Aeronautics: Outer Planet Entry Heating and Thermal Protection, Vol. 64, R. Viskanta (ed.), page 65 (1979).
- L. Biolsi and K. J. Biolsi
"Transport Properties of Monatomic Carbon II: Contributions from Excited Electronic States"
Journal of Geophysical Research, 84, 5311 (1979).
- L. Biolsi
"Proposed Computational Method for Transport Properties of Ablation Products"
American Institute of Aeronautics and Astronautics Journal (in press).

Presentations

- L. Biolsi
"Effect of Surface Ablation on Transport Properties in a H₂-He Atmosphere"
173rd National Meeting, American Chemical Society
New Orleans, LA, March 20-25, 1977.
- L. Biolsi
"Transport Properties in the Atmosphere of Jupiter"
13th Midwest Regional Meeting, American Chemical Society
Rolla, MO, Nov. 3-4, 1977.
- L. Biolsi
"Transport Properties of Gaseous Carbon"
33rd Southwest Regional Meeting, American Chemical Society
Little Rock, AR, Dec. 5-7, 1977.
- L. Biolsi
"Some Effects of Ablation on Transport Properties in the Jovian Atmosphere"
2nd AIAA/ASME Thermophysics and Heat Transfer Conference
Palo Alto, CA, May 24-26, 1978.
- L. Biolsi and K. J. Biolsi
"The Thermal Conductivity of Carbon in Electronically Excited States"
14th Midwest Regional Meeting, American Chemical Society
Fayetteville, AR, Oct. 26-27, 1978.

- L. Biolsi and L. R. Wallace
"Transport Properties in a C_2 -C System"
14th Midwest Regional Meeting, American Chemical Society
Fayetteville, AR, Oct. 26-27, 1978.
- L. Biolsi
"Inelastic Cross Sections for Ion-Diatomic Molecule Interactions"
53rd Colloid and Surface Science Symposium
Rolla, Missouri, June 11-13, 1979.
- L. Biolsi and J. Fenton
"Transport Properties in a Gaseous Mixture of C and C_2 "
178th National Meeting, American Chemical Society
Washington, D.C., September 9-14, 1979.
- B. Owenson and L. Biolsi
"Transport Properties Associated with Photochemical Smog"
15th Midwest Regional Meeting, American Chemical Society
St. Louis, Missouri, November 8-9, 1979.